

Ionic Association in $\text{CH}_3-(\text{CH}_2-\text{CF}_2)_n-\text{CH}_3(\text{PVDF})-\text{Li}^+-\text{N}^-(\text{CF}_3\text{SO}_2)_2$ for $n = 1, 4$: A Computational Approach

Mathew Daniel, Susan G. Duggan, Kyung Seol, Gregory J. McManus, and Nilesh R. Dhupal*

Cite This: *ACS Omega* 2022, 7, 7116–7124

Read Online

ACCESS |



Metrics & More

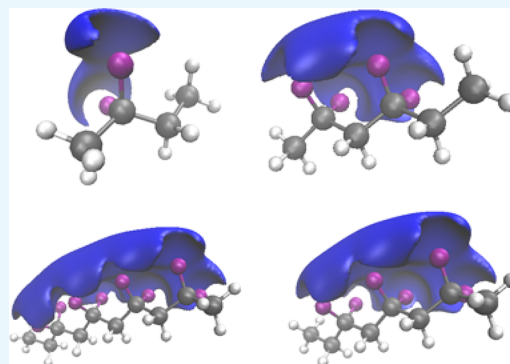


Article Recommendations



Supporting Information

ABSTRACT: The ionic conductivity of solid polymer electrolytes is governed by the ionic association caused by the polymer...Li⁺ and the anion...Li⁺ interactions. We performed the density functional calculation to analyze the molecular interactions in the $\text{CH}_3-(\text{CH}_2-\text{CF}_2)_n-\text{CH}_3-\text{Li}^+-\text{N}^-(\text{CF}_3\text{SO}_2)_2$ for $n = 1, 4$ systems. The gauche conformation is predicted in the lowest energy conformer of pure polymer except for $n = 1$. The lithium coordination number with the polymer is changed from 3 to 2 in the presence of anion for $n = 2, 4$ systems. The consequences of the Li⁺ ion and Li⁺-(CF₃SO₂)₂N⁻ to the vibrational spectrum are studied to understand the ionic association at the molecular level.



INTRODUCTION

Lithium-ion batteries (LIBs) are used as commercial electrochemical energy storage devices in mobile phones, laptops, electric cars, and a variety of other electronic products. Electrolytes play an important role in determining the performance of the battery. However, certain safety issues arise from the use of liquid electrolytes in traditional LIBs: these issues, which include the flammability of many organic solvents and electrolyte leakage, severely limit the application of LIBs on a larger scale.¹ The solid polymer electrolytes (SPEs) can be a safer alternative to liquid electrolytes.

The SPEs have received wide attention because of their advantages of mechanical superiority, flexibility, high energy density, and thermal safety compared to liquid electrolytes.^{2–4} The polymer host itself is used as a solid solvent, along with lithium salt in SPEs and does not contain any organic liquids. The first reported study of SPEs was composed of poly(ethylene oxide) (PEO) and alkali metal.⁵ The important aspect of SPEs composed of PEO is understanding the ion transport phenomena by analyzing the interaction between the metal (Li⁺) ion and the ether oxygen atoms of PEO.⁶ The ionic conductivity of the SPEs are mainly governed by the functional group of the polymer chain which coordinates with the lithium-ion of salt. The ionic association attributed to the intermolecular interactions such as the ion–polymer and ion–anion interactions of the systems play an important role in the ion transport phenomenon in SPEs.^{7,8} In addition to ionic association, the segmental motion of the polymer that arises from the conformational change in the polymer backbone due to metal–polymer interactions also play equally important role in governing the ionic conductivity of the polymer. Thus, the ionic

conductivity of the SPEs can be understood by the information about the local structure of the polymer matrix. Ab initio quantum chemical calculations are used extensively to understand the relationship between the ionic conductivity and the local structure of the polymer matrix at the molecular level.^{7,9,10}

Polar polymers such as poly(vinylidene fluoride) (PVDF) and poly(ethylene oxide) are good materials for solid or gel electrolytes in secondary lithium-ion batteries.¹¹ The strong electron-withdrawing groups in PVDF can provide effective ion conduction through the polymer–Li⁺ ion interactions.^{12–14} The ionic conductivity of these polymers mainly depend upon the coordination of Li⁺ ion to electronegative atoms such as oxygen in PEO and fluorine atoms in PVDF atoms of polymer and subsequent changes in the polymer conformation. The ionic association in these polymers occurs via the consequences of Li⁺–polymer interactions because of the weakening of cation–anion interactions. The degree of dissociation of the metal (Li⁺) ion from the anion influence the ionic conductivity of the polymer. Quantum chemical calculations were employed to understand the local coordination of the mono- and divalent cations, and the normal vibrational frequencies of the system composed on the different chain lengths of PEO, H₃CO–(CH₂–CH₂–O)_n–CH₃ ($n = 2–7$).^{15–17} The weakening of the carbon–oxygen bond in the PEO–cation complex with respect

Received: December 1, 2021

Accepted: February 3, 2022

Published: February 15, 2022



to free PEO can be correlated with the cation-binding strengths with the ether oxygen atoms and a subsequent downshift is predicted for C–O–C stretching vibration. The stronger molecular interactions of polymer with Li^+ ion of the ion pair (comprised of Li^+ and anion) can consequently weaken of the Li^+ anion interactions in the ion pair.^{18–20} The degree of dissociation of anion from Li -ion can improve the ionic conductivity of the electrolytes.

With this view, we study the ionic association in terms of the electronic structure and the normal vibrations in $\text{CH}_3-(\text{CH}_2-\text{CF}_2)_n-\text{CH}_3-\text{Li}^+(\text{CF}_3\text{SO}_2)_2\text{N}^-$ electrolytes by performing the ab initio quantum chemical calculations. Consequences of the molecular interactions to vibrational spectrum are studied by assigning the normal vibrations and the frequency shift of intense vibrations. The computational method has been outlined next.

RESULTS AND DISCUSSION

Different conformers of the $\text{CH}_3-(\text{CH}_2-\text{CF}_2)_n-\text{CH}_3$ ($n = 1-4$) polymer units were generated by rotation between two C–C–C planes. If the angle between two planes is around 0° or 180° , it is referred to as trans, and angles around 60° or 120° are referred to as gauche. The conformers can be distinguished based on the gauche and trans conformation of the polymer backbone. Selected conformers of $\text{CH}_3-(\text{CH}_2-\text{CF}_2)_n-\text{CH}_3$ ($n = 1-4$) are shown in Figure 1 and 2. The electronic energy and relative stabilization energy of conformers of $\text{CH}_3-(\text{CH}_2-\text{CF}_2)_n-\text{CH}_3$ ($n = 1-4$) are compared in Table 1. The zero-point corrected electronic energy and relative stabilization energy of conformers of $\text{CH}_3-(\text{CH}_2-\text{CF}_2)_n-\text{CH}_3$ ($n = 1-4$) are also compared in Table S1 in Supporting Information. The relative

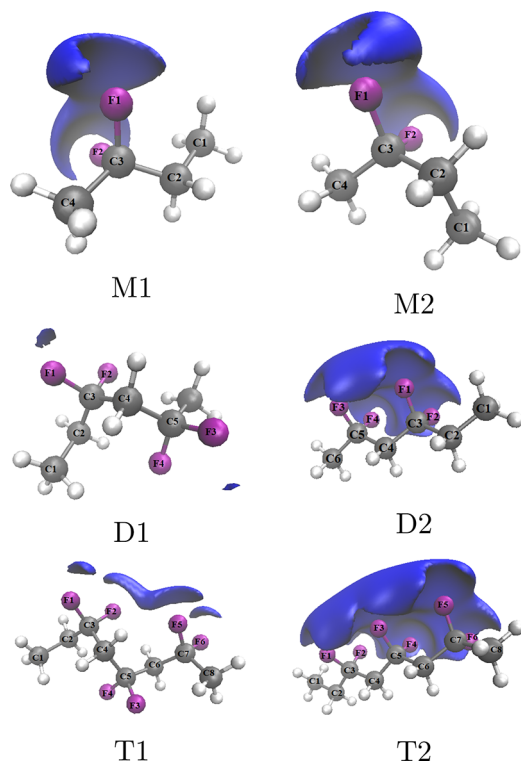


Figure 1. MESP iso-surface ($V = -81.4 \text{ kJ mol}^{-1}$) of different conformers of $\text{CH}_3-(\text{CH}_2-\text{CF}_2)_n-\text{CH}_3$ ($n = 1-3$). Carbon, hydrogen, and fluorine atoms are shown in dark gray, white, and purple, respectively.

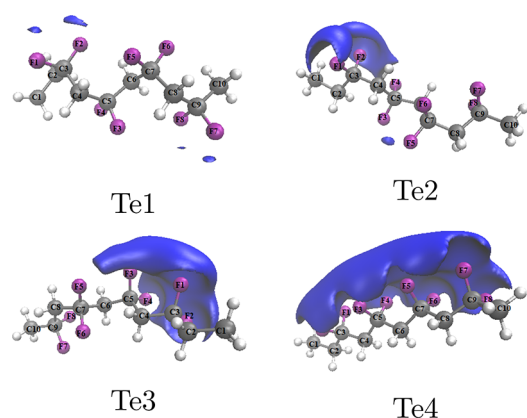


Figure 2. MESP iso-surface ($V = -81.4 \text{ kJ mol}^{-1}$) of different conformers of $\text{CH}_3-(\text{CH}_2-\text{CF}_2)_4-\text{CH}_3$.

Table 1. Electronic (E in au) and Relative Stabilization Energy (ΔE in kJ/mol) of conformers of $\text{CH}_3-(\text{CH}_2-\text{CF}_2)_n-\text{CH}_3$ ($n = 1-4$)

system	E	ΔE
M1	−356.952 197	0.00
M2	−356.951 410	2.07
D1	−634.062 481	0.00
D2	−634.056 667	15.26
T1	−911.171 537	0.00
T2	−911.160 573	28.79
Te1	−1188.281 033	0.00
Te2	−1188.276 973	10.66
Te3	−1188.273 788	19.02
Te4	−1188.264 380	43.72

stabilization energy difference between two conformers is around 2 kJ/mol within B3LYP/6-31G** methods. We performed the calculations for these two conformers using different methods and basis sets. The electronic energy calculated using different methods is summarized in Table S2. Our previous study has shown that the B3LYP results are agreed well with the experimental results.^{21–23} Here, we present the results calculated using the B3LYP/6-31G** method. We labeled $n = 1$, $n = 2$, $n = 3$, and $n = 4$ in $\text{CH}_3-(\text{CH}_2-\text{CF}_2)_n-\text{CH}_3$ as M, D, T, and Te, respectively. The Li^+ ion complex with these polymer units are represented as C1, C2, C3, and C4 for n value 1, 2, 3, and 4 respectively.

We studied MESP to analyze the effective localization of the electron-rich regions around the fluorine atoms in the molecular system. MESP isosurfaces ($V = -81.4 \text{ kJ mol}^{-1}$) of different $\text{CH}_3-(\text{CH}_2-\text{CF}_2)_n-\text{CH}_3$ ($n = 1-4$) conformers are depicted in Figures 1 and 2. As it may be noticed readily within the conformers of the series, the volume enclosed by the MESP isosurface for trans conformation is relatively larger compared to those in corresponding gauche conformers. In terms of electron density, the electron density that arises from the fluorine atoms is more localized or dense in trans conformation than gauche conformation. In other words, the electron density is added together from each CF_2 groups in trans conformation whereas the electron density is subtracted in gauche conformation. The relative position of CF_2 groups in the gauche conformer makes it energetically stable compared to the trans conformer. The CF bond distance in trans conformation is relatively shorter compared to that in gauche conformation. The stronger bond in trans conformation may be due to a transfer of the electron

density from fluorine atoms to the CF bonds of CF₂ groups to minimize the repulsion between CF₂ groups. We compared the CF distance of different conformers for CH₃-(CH₂-CF₂)_n-CH₃ (*n* = 1–4) in Table 2.

Table 2. Comparison of CF Distance (in Å) with in Different Conformers of CH₃-(CH₂-CF₂)_n-CH₃-Li⁺ (*n* = 1–4)^a

system	C3F1	C3F2	C5F3	C5F4	C7F5	C7F6
M1	1.382	1.382				
M2	1.383	1.382				
D1	1.381	1.385	1.386	1.379		
D2	1.377	1.376	1.374	1.376		
T1	1.381	1.384	1.384	1.383	1.382	1.379
T2	1.377	1.375	1.369	1.369	1.373	1.376
Te1	1.381	1.385	1.381	1.382	1.383	1.382
Te2	1.385	1.377	1.379	1.379	1.378	1.380
Te3	1.377	1.385	1.370	1.377	1.388	1.378
Te4	1.374	1.377	1.369	1.369	1.369	1.369

^aC9–F7 = Te1, 1.384; Te2, 1.385; Te3, 1.384; Te4, 1.376. C9–F8 = Te1, 1.379; Te2, 1.376; Te3, 1.376; Te4, 1.373.

Experimentally, three crystalline phases, α , β , and γ of poly(vinylidene fluoride) are studied under distinct crystallization conditions. The gauche conformation is observed in the α phase and the trans conformation in the β phase. Both gauche and trans conformations are present in the γ phase. The highest dipole moment is observed for the β phase based on the morphology whereas the lower dipole moment is observed for the non polar α phase due to the antiparallel packing of the dipoles within the unit cells. These observation is consistent with the interference drawn from the MESP isosurface of the different structures. Nishiyama²⁴ et. al studied the crystalline structure of the PVDF with the antisolvnet addition method. The crystalline structure of PVDF studied by the melting and solvent evaporation method preferred the phase. The intermolecular interactions energy study of PVDF revealed that the α phase is stable than the β phase in terms of potential energy. These experimental results agree well with the simulation results.

We investigated the interaction of Li⁺ and Li⁺-Tf₂N⁻ ion pair with polymer to understand the ionic association mechanism at the molecular level. The MESP isosurface are used as a binding site of cation to the polymer. We placed Li⁺ or Li⁺-Tf₂N⁻ near fluorine sites of the polymers according to the results of MESP isosurface to investigate the interactions of model polymers with Li⁺ and Li⁺-Tf₂N⁻ salt.

The ionic association in SPE is a consequence of the interactions between the polymer and Li⁺ ion or Li⁺-Tf₂N⁻ salt. The CF bond distance and F...Li⁺ in CH₃-(CH₂-CF₂)_n-CH₃-Li⁺ (*n* = 1–4) systems are compared in Tables 3 and 4 respectively. Optimized geometries of different conformers of Li⁺-CH₃-(CH₂-CF₂)_n-CH₃ (*n* = 1–4) are shown in Figures S1 and S2. The CF elongation is predicted for CF bond interacting Li⁺ ion compared to the free state. On the other, the bond shortening is noticed for the CF bond not participating in the interactions. The Li⁺ ion coordinates with two or three fluorine atoms of the polymer. The trans conformation is predicted in the lowest energy conformation of *n* = 1 and 2, whereas the gauche conformation is preferred in the lowest energy Li-polymer conformers of *n* = 3 and 4. The stability of the lowest energy is depends on the coordination of Li⁺ ion, as well as the interaction strength between the Li⁺ and fluorine atom of polymer. It should be noted here that no systematic

Table 3. Comparison of CF Distance (in Å) within Different Conformers of Li⁺-CH₃-(CH₂-CF₂)_n-CH₃ (*n* = 1–4)^a

system	C3F1	C3F2	C5F3	C5F4	C7F5	C7F6
C11	1.439	1.439				
C12	1.441	1.441				
C21	1.421	1.417	1.454	1.355-		
C22	1.442	1.443	1.380-	1.366-		
C31	1.489*	1.350	1.370	1.372	1.421*	1.425*
C32	1.454*	1.355	1.412*	1.411*	1.370	1.383
C41	1.454*	1.359	1.434*	1.350	1.448	1.362
C42	1.383	1.367	1.371	1.370	1.420	1.430
C43	1.453	1.355	1.411	1.411	1.364	1.380
C44	1.370	1.375	1.342	1.468	1.409	1.428

^aC9–F7 = C41, 1.378; C42, 1.488; C43, 1.372; C44, 1.377. C9–F8 = C41, 1.383; C42, 1.349; C43, 1.374; C44, 1.382.

Table 4. Comparison of CF Distance (in Å) with in Different Conformers of Li⁺-CH₃-(CH₂-CF₂)_n-CH₃ (*n* = 1–4)^a

system	F1...Li ⁺	F2...Li ⁺	F3...Li ⁺	F4...Li ⁺	F5...Li ⁺	F6...Li ⁺
C11	1.891	1.891				
C12	1.891	1.889				
C21	1.980	1.982	1.856			
C22	1.900	1.887				
C31	1.820				1.967	2.004
C32	1.885		1.960	1.966		
C41	1.846		1.877		1.884	
C42			1.954	2.038		
C43	1.891		1.955		1.971	
C44			1.827		2.057	1.933

^aC42: F6...Li⁺, 1.821.

trend is observed between the lithium...fluorine interaction strength and inferences drawn from the MESP isosurface like in poly(ethylene oxide) (PEO) and perfluoropolyether (PFPE) polymer.^{16,25} The symmetric lithium...fluorine distance is predicted in M1–Li conformer. The Li⁺ ion is preferred to interact strongly with the fluorine atom of CF₂ group attached to the terminal CH₃ group compared to other two fluorine atoms. The stronger interaction of Li⁺ ion with CF₂ group attach to the terminal CH₃ groups may be due to the more electronegativity of fluorine atom through the electron donating inductive effect of CH₃ group.

The choice of the anion of lithium salt play an important role in the ionic association of SPE. The CF, F...Li⁺, and O...Li⁺ in CH₃-(CH₂-CF₂)_n-CH₃-Li⁺ (*n* = 1–4) and anion bond distance systems are compared in Tables 5–8. Optimized geometries of different conformers of Li⁺-Tf₂N⁻-CH₃-(CH₂-CF₂)_n-CH₃ (*n* = 1–4) are displayed in Figures 33 and 4. As expected, the Li⁺ ion interactions with the polymer gets weaker in the presence of the anion and consequently the Li⁺ ion interactions gets weaker with the anion in the presence of polymer. These relative changes in the interactions are the fundamental of the ionic association. For example, the interaction of the polymer with Li⁺ ion results in an increase in the CF bond distance approximately by 0.057 Å, whereas the increase in the CF bond distance is lowered to 0.029 Å in the presence of anion for *n* = 1 polymer unit. The weakening of the distance between the Li⁺ ion and polymer is approximately by 0.310 Å in the presence of anion. The consequent change in the distance between the Li⁺ ion and the anion in the presence of polymer is 0.042 Å. Thus, the separation of the anion from the

Table 5. Comparison of CF Distance (in Å) within Different Conformers of $\text{Li}^+-\text{Tf}_2\text{N}^--\text{CH}_3-(\text{CH}_2-\text{CF}_2)_n-\text{CH}_3$ ($n = 1-4$)^a

system	C3F1	C3F2	C5F3	C5F4	C7F5	C7F6
C11-Tf ₂ N ⁻	1.411	1.411				
C12-Tf ₂ N ⁻	1.412	1.411				
C21-Tf ₂ N ⁻	1.415	1.368	1.416	1.361		
C22-Tf ₂ N ⁻	1.386	1.373	1.412	1.413		
C31-Tf ₂ N ⁻	1.427	1.365	1.379	1.380	1.425	1.364
C32-Tf ₂ N ⁻	1.422	1.362	1.417	1.356	1.377	1.374
C41-Tf ₂ N ⁻	1.376	1.1.386	1.420	1.1.369	1.377	1.379
C42-Tf ₂ N ⁻	1.412	1.366	1.390	1.369	1.404	1.370
C43-Tf ₂ N ⁻	1.377	1.380	1.425	1.360	1.420	1.362
C44-Tf ₂ N ⁻	1.374	1.377	1.368	1.371	1.355	1.417

^aC9-F7 = C41-Tf₂N⁻, 1.431; C42-Tf₂N⁻, 1.377; C43-Tf₂N⁻, 1.384; C44-Tf₂N⁻, 1.360. C9-F8 = C41-Tf₂N⁻, 1.376; C42-Tf₂N⁻, 1.363; C43-Tf₂N⁻, 1.376; C44-Tf₂N⁻, 1.422.

Table 6. Comparison of Li⁺...F Distance (in Å) within Different Conformers of $\text{Li}^+-\text{Tf}_2\text{N}^--\text{CH}_3-(\text{CH}_2-\text{CF}_2)_n-\text{CH}_3$ ($n = 1-4$)^a

system	F1...Li ⁺	F2...Li ⁺	F3...Li ⁺	F4...Li ⁺	F5...Li ⁺
C11-Tf ₂ N ⁻	2.024	2.021			
C12-Tf ₂ N ⁻	2.024	2.026			
C21-Tf ₂ N ⁻	1.963		1.965		
C22-Tf ₂ N ⁻			2.037	2.035	
C31-Tf ₂ N ⁻	1.965				1.973
C32-Tf ₂ N ⁻	1.929		1.962		
C41-Tf ₂ N ⁻			1.995		
C42-Tf ₂ N ⁻	2.000		2.209		2.051
C43-Tf ₂ N ⁻			1.959		1.942
C44-Tf ₂ N ⁻					

^aC41: F7...Li⁺, 1.956. C44: F6...Li⁺, 1.927. C44: F8...Li⁺, 1.953.

Table 7. Comparison of Li⁺...O Distance (in Å) in Different Conformers of $\text{Li}^+-\text{Tf}_2\text{N}^--\text{CH}_3-(\text{CH}_2-\text{CF}_2)_n-\text{CH}_3$ ($n = 1-4$)^a

system	Li ⁺ ...O12	Li ⁺ ...O22
C11-Tf ₂ N ⁻	1.850	1.853
C12-Tf ₂ N ⁻	1.846	1.861
C21-Tf ₂ N ⁻	1.870	1.870
C22-Tf ₂ N ⁻	1.843	1.865
C31-Tf ₂ N ⁻	1.860	1.860
C32-Tf ₂ N ⁻	1.863	1.907
C41-Tf ₂ N ⁻	1.859	1.862
C42-Tf ₂ N ⁻	1.903	1.890
C43-Tf ₂ N ⁻	1.854	1.875
C44-Tf ₂ N ⁻	1.864	1.911

^aO...Li: 1.810. O...Li: 1.810.

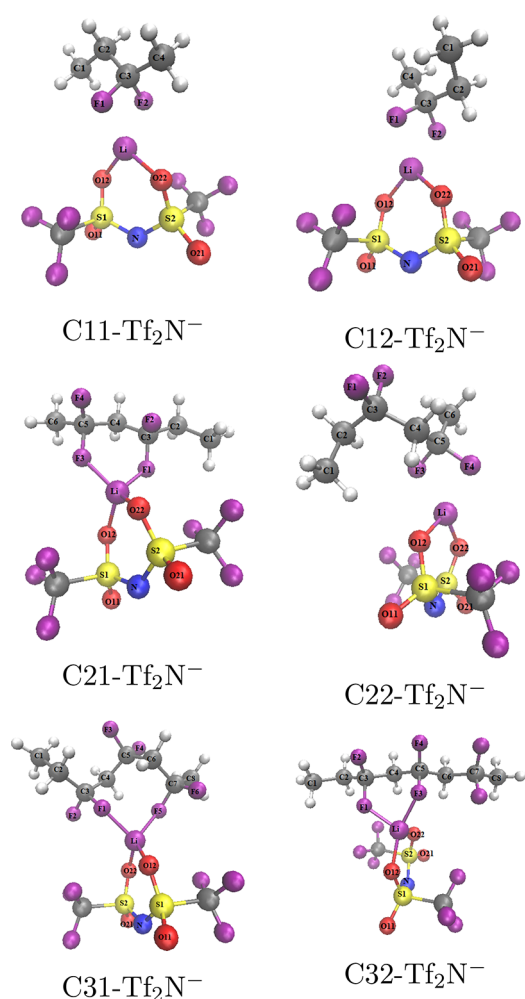
Li⁺ ion in the presence polymer is relatively less significant in terms of distance compared to the change in the distance between the Li⁺ ion and fluorine atoms of the polymer, which may result in the weak ionic association for $n = 1$ polymer unit.

The change in the coordination number of the Li⁺ ion from 3 to 2 is predicted for most of the conformer in the presence of anion. The maximum bond elongation of 0.105 Å is predicted for the CF bond in the C31 conformer with respect to the CF bond in the C41 conformer. The anion presence reduces the bond elongation by 0.067 Å in the T1-Li-Tf₂N conformer.

Table 8. Comparison of Anion Distance (in Å) of Free Tf₂N^{-a} and Li⁺-Tf₂N^{-b} in Different Conformers of $\text{Li}^+-\text{Tf}_2\text{N}^--\text{CH}_3-(\text{CH}_2-\text{CF}_2)_n-\text{CH}_3$ ($n = 1-4$)

system	S1N	2SN	S1O11	S1O12	S2O21	S2O22
C11-Tf ₂ N ⁻	1.609	1.609	1.454	1.498	1.454	1.498
C12-Tf ₂ N ⁻	1.608	1.610	1.454	1.498	1.453	1.498
C21-Tf ₂ N ⁻	1.609	1.611	1.454	1.495	1.455	1.495
C22-Tf ₂ N ⁻	1.606	1.611	1.454	1.500	1.453	1.498
C31-Tf ₂ N ⁻	1.609	1.609	1.454	1.496	1.454	1.496
C32-Tf ₂ N ⁻	1.599	1.618	1.455	1.500	1.453	1.494
C41-Tf ₂ N ⁻	1.611	1.608	1.454	1.496	1.454	1.495
C42-Tf ₂ N ⁻	1.610	1.611	1.455	1.492	1.455	1.493
C43-Tf ₂ N ⁻	1.606	1.611	1.454	1.500	1.453	1.496
C44-Tf ₂ N ⁻	1.619	1.600	1.453	1.494	1.455	1.500

^aS1N, 1.602; S2N, 1.602; S1O11, 1.469; S1O12, 1.468; S2O21, 1.469; S2O22, 1.468. ^bS1N, 1.606; S2N, 1.606; S1O11, 1.452; S1O12, 1.504; S2O21, 1.452; S2O22, 1.504.

**Figure 3. Optimized geometries of different conformers of $\text{Li}^+-\text{Tf}_2\text{N}^--\text{CH}_3-(\text{CH}_2-\text{CF}_2)_n-\text{CH}_3$ ($n = 1-3$).**

The anion not only reduces the interaction strength with the Li⁺ ion but also changed the coordination number of the Li⁺ ion. The larger weakening of the Li⁺ ion interaction with polymer in the presence of anion compared to the interaction of the Li⁺ ion with anion in the presence of polymer may result in the lower conductivity.

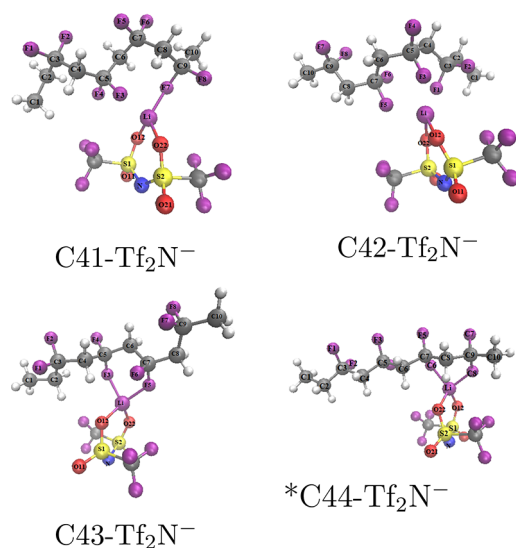


Figure 4. Optimized geometries of different conformers of $\text{Li}^+ - \text{Tf}_2\text{N}^- - \text{CH}_3 - (\text{CH}_2 - \text{CF}_2)_4 - \text{CH}_3$.

We compared the bond distances of anion for free anion, $\text{Li}^+ - \text{Tf}_2\text{N}^-$ ion pair, and the polymer conformer in Table 8. The bond distance for SO bond participating in the interaction with Li^+ is relatively longer compared to non participating SO bonds. The bond distance of SO participating in the interaction for the lowest energy conformer of $\text{CH}_3 - (\text{CH}_2 - \text{CF}_2)_n - \text{CH}_3 - \text{Li}^+ - \text{Tf}_2\text{N}^-$ ($n = 1-4$) ranges from 1.495 to 1.500 Å. The average decrease in the bond of these SO bonds is by 0.007 Å in the presence of polymer which is less significant in terms of disassociation of the Li^+ ion from the anion. Thus, the stronger interaction between the anion and the Li^+ in the presence of polymer compared to the interaction between the Li^+ ion and polymer in presence anion makes the anion dissociation difficult.

Vibrational frequency analysis can provide microscopic information about the structure and the ionic interactions of the system. The consequences of the molecular interactions manifest in the vibrational spectrum and result in the frequency shifts of the normal vibrations. The interpretation of these interactions may be a difficult task in the experimental spectrum. A good approach is to perform quantum chemical calculations to calculate the normal vibrations and compare those with the experimental spectrum. This combined approach of comparison of simulated vibration spectra with the experiment helps in assigning the vibrations of experimental spectra. Experimentally, three crystalline phases, α , β , and γ of poly(vinylidene fluoride) are studied under distinct crystallization conditions and infrared absorption bands able to identify the presence of the different phases. With this view, we investigated the normal vibrational frequency analysis of the lowest energy conformer of pure polymer, Li^+ -polymer, and $\text{Li}^+ - \text{Tf}_2\text{N}^-$ -polymer for $n = 1-4$ to study the possible change in the conformation of the polymer after interacting with the cation. The vibrational frequencies are presented in the Tables 9 and 10, and these harmonic frequencies are scaled by 0.97²⁶⁻³⁰ scaling factor.

The relatively high number of characteristics bands of the α phase helps to identify the presence in the experiment. The experimental absorption bands at 489, 614, 766, 795, 855, and 976 cm^{-1} are assigned to identify the presence of the α phase experimentally. The vibration around 985 cm^{-1} assigned to the CH_2 twist vibration in D1, T1, and Te1 can be correlated with the experimental vibration observed at 976 cm^{-1} . The

absorption band at 795 cm^{-1} in the experimental spectrum can be correlated with the symm CC stretch predicted at 794, 785, and 781 in D1, T1, and Te1, respectively. The CF_2 wag vibration predicted in the range of 540–550 for D1, T1, and Te1 can be compared with the 532 absorption band of the experimental IR spectrum. The intense vibrations around 1233 assigned to CH_2 twist vibrations can be correlated with the 1232 absorption band of γ phase. The absorption band at 812 of γ phase can be correlated with the 828 and 838 vibrations of T1 and Te1 respectively. The major α phase characteristics vibrations are predicted in the simulation vibrational spectrum and the minor presence of γ phase is predicted based on the compression with the experimental spectrum. It should be remarked here that the γ is a mixture of α and β phases. The presence of the characteristics absorption band of the β and the γ phases depend on the population of trans and gauche present in the conformation.

The change in the intensity is predicted for the CH_3 rocking vibration on cation coordination with polymer. No systematic trend is predicted for this vibration with cation interaction or increase in the chain length. Similar to CH_3 rocking, the SO stretching of non participating in the interactions are predicted around 1282 and 1264 cm^{-1} in all lowest energy structures of $n = 1, 4$. This vibrations are predicted at 1284 and 1266 cm^{-1} in $\text{Li}^+ - \text{Tf}_2\text{N}^-$ ion pair. It can be inferred that the effect of polymer–lithium ion interaction on this SO vibration in terms of frequency shift is less significant due to weak polymer $\cdots\text{Li}^+$ ion interactions. In addition to SO vibrations, the CH_2 bending vibrations such as CH_2 rocking, twisting are also relatively less sensitive to the polymer–lithium interactions. Interestingly, the symmetric SO_2 stretch vibrations are predicted at 1167, 1049, and 1050 cm^{-1} for mono, tri, and tetra, respectively which is absent for $n = 2$. A correlation between the SO bond distance (SO bond participating in the interaction with lithium-ion) and the frequency shift to lower wavenumber is predicted for the asymmetric SO_2 vibration coupled with SN stretching vibration. Intense vibrations at 1047 and 1039 cm^{-1} in the lowest energy conformer of $n = 1$ and 2, respectively, are assigned to SN and SO_2 stretching vibration, whereas the same vibration is predicted at 1012 cm^{-1} in the lowest energy conformer of $n = 3$ and 4. Thus, the frequency analysis predicted the similar inferences that the ionic association is less favorable due to weak $\text{F}\cdots\text{Li}^+$ interactions.

An SN stretch coupled with SO_2 stretch vibration at 1034 cm^{-1} is only predicted in the lowest energy conformer of $n = 1$ whereas the vibration around 982 cm^{-1} assigned to the same vibration is observed in all polymer unit ($n = 1-4$). The vibration associated with $\text{F}-\text{Li}$ is shifted to a higher wavenumber in the presence of anion due to the weakening of polymer–lithium interactions in the presence of anion. The vibration at 657 cm^{-1} in $\text{Li}^+ - \text{Tf}_2\text{N}^-$ ion pair is assigned to $\text{Li}\cdots\text{O}$ stretching. This vibration is red-shifted in the presence of polymer due to the weakening of the lithium anion interaction. The SO stretching vibration for SO bond participating in the present study is predicted at a lower wavenumber compared to those in the PEO polymer report in ref 25. This can be inferred that the polymer interactions with lithium-ion in the presence of anion are stronger compared to the interactions predicted in the present study. Thus, the vibrational frequency can provide the molecular picture of the ionic association in the solid polymer electrolytes.

Table 9. Comparison of the Selected Vibrational Frequencies (in cm^{-1}) of M1, C11, C11– Tf_2N^- , D1, C21, and C21– Tf_2N^- Structures^a

vibrations	M1	C11	C11– Tf_2N^-	D1	C21	C21– Tf_2N^-
CH ₃ rocking	1389 (24)	1399 (40)	1397 (29)	1395 (34)	1397 (57)	1393 (53)
CH ₂ rock				1363 (67)	1378 (57)	1377 (56)
CH ₂ rock				1355 (36)		
SO ₂ symm stretch			1283 (432)			1283 (414)
CH ₂ twist	1287 (26)				1310 (80)	1310 (112)
SO ₂ asymm stretch			1271 (313)			1271 (327)
CH ₂ twist	1234 (79)			1232 (67)		1231 (85)
CC stretch + CH ₂ rock		1215 (58)	1223 (103)	1228 (81)	1216 (60)	
CH ₂ twisting + CF stretching						1230 (83)
CH ₂ twisting + CF stretching						1229 (320)
CH ₂ twist + CF stretch						1210 (54)
CH ₂ twist					1192 (74)	
CH ₂ twist	1180 (74)		1176 (47)	1181 (85)		
CF stretch + CH ₃ twist	1180 (56)	1158 (72)		1180 (113)	1165 (122)	
CH ₂ wag						1172 (38)
CH ₂ twist						1159 (205)
CC stretch + CF stretch						1148 (69)
asymm CC stretch				1115 (84)		
CH ₂ twist		1130 (42)	1148 (34)		1136 (66)	1100 (38)
CH ₂ twist + CF stretch						1071 (20)
symm SO ₂ stretch*			1167 (189)			
CH ₂ twist	1043 (23)		1035 (109)	1028 (17)		
asymm SO ₂ + SN stretch			1164 (197)			1051 (126)
symm CC stretch	1031 (19)	1025 (31)			1024 (20)	
CH ₂ twist		1016 (19)				
CH ₂ twist				987 (81)		
SN + SO ₂ stretch			1047 (98)			1039 (305)
CH ₃ + CH ₂ wag						1032 (30)
SN + SO ₂ stretch			1034 (334)			
SN + SO ₂ stretch			982 (525)			983 (544)
CH ₂ wag						972 (57)
CH ₂ wag				966 (23)	957 (33)	957 (29)
CH ₂ wag				951 (24)	948 (34)	941 (16)
CH ₂ wag				928 (43)		
CH ₂ wag	911 (17)			876 (25)		886 (14)
CF stretch	915 (70)	887 (44)				
CF stretch + CH ₂ wag			853 (82)			857 (78)
CF stretch + CH ₂ wag		806 (97)				785 (36)
symm CC stretch				794 (13)		
CH ₂ wag		728 (57)				768 (41)
symm CC + CF stretch		701 (25)				
O...Li vibration			612 (102)			598 (78)
O...Li vibration						591 (51)
symm O–Li–O stretch			598 (73)			579 (69)
F...Li vibration			583 (43)			568 (322)
CF ₂ wag		553 (20)			543 (36)	543 (22)
SNSOLiO ring vibration						524 (31)
CF ₂ wag				540 (17)	522 (30)	518 (34)
O–Li–O bend						496 (71)
F...Li vibration		447 (147)			448 (80)	

^aThe intensities (in km/mol) are given in parentheses.

CONCLUSIONS

Systematic investigation of the structure and normal frequencies of the $\text{CH}_3-(\text{CH}_2-\text{CF}_2)_n-\text{CH}_3-\text{Li}^+(\text{CF}_3\text{SO}_2)_2\text{N}^-$ for $n = 1, 4$ systems by employing quantum chemical calculations. MESP surfaces revealed that the relatively large distance between the CF_2 minimizes in the gauche conformation preferred in the lowest energy conformer compared to trans conformation

except for $n = 1$. The MESP results correlated well with the experimental dipole moment trend. The ionic interactions between Li^+ ion and the polymer unit result in the CF distance elongation whereas a consequent decrease in the bond distance is noticed for the same CF bonds in the presence of anion. The weak interactions of the Li^+ ion with the polymer unit unable the dissociation of the $\text{Li}^+(\text{CF}_3\text{SO}_2)_2\text{N}^-$ ion pair. The con-

Table 10. Comparison of the Selected Vibrational Frequencies (in cm^{-1}) of T1, C31, C31– Tf_2N^- , Te1, C41, C41– Tf_2N^- Structures^a

vibrations	T1	C31	C31– Tf_2N^-	Te1	C41	C41– Tf_2N^-
CH ₃ rocking	1394 (21)	1395 (31)	1398 (28)	1395 (21)	1395 (74)	1399 (32)
CH ₂ rock					1392 (26)	
CH ₂ rock					1390 (54)	
CH ₂ rock	1369 (82)	1376 (90)	1372 (78)	1374 (28)	1374 (103)	1375 (44)
CH ₂ rock	1363 (33)			1371 (48)		1369 (17)
CH ₂ rock			1365 (56)	1358 (134)		1360 (150)
CH ₂ rock	1353 (77)	1355 (71)	1350 (43)	1354 (72)	1359 (50)	1353 (61)
CH ₂ twist	1305 (14)	1336 (32)	1286 (43)	1299 (30)	1314 (23)	1298 (33)
SO ₂ symm stretch			1282 (222)			1282 (387)
CH ₂ twist	1286 (25)	1281 (39)	1281 (244)		1264 (47)	1281 (83)
CH ₂ twist	1279 (11)					
SO ₂ asymm stretch			1263 (319)			1264 (297)
CH ₂ twist	1233 (26)	1231 (52)	1233 (142)	1235 (39)	1233 (149)	
CC stretch + CH ₂ rock	1229 (86)	1218 (53)	1228 (44)	1230 (58)	1222 (75)	1235 (46)
CH ₂ twisting + CF stretching			1230 (221)			1234 (168)
CH ₂ twisting + CF stretching			1230 (94)			1228 (125)
CH ₂ twist + CF stretch	1216 (123)	1206 (144)	1199 (405)	1215 (86)	1213 (202)	1214 (133)
CH ₂ twist + CF stretch				1212 (158)		1199 (284)
CH ₂ twist	1186 (185)	1189 (32)	1195 (23)	1189 (179)	1191 (99)	1196 (40)
CH ₂ twist			1193 (97)			1185 (50)
CF stretch + CH ₃ twist	1180 (69)	1150 (172)		1180 (104)	1166 (122)	1183 (97)
CH ₂ wag			1192 (29)			1170 (36)
SC stretch + CH ₂ wag			1170 (89)			1166 (283)
Sn + SC stretch + CH ₂ wag			1165 (173)			1162 (262)
CH ₂ twist	1147 (26)			1162 (192)	1140 (57)	1158 (196)
asymm CC stretch			1146 (95)			
asymm CC stretch					1123 (58)	
CH ₂ twist		1110 (71)			1102 (34)	
CH ₂ twist	1090 (136)				1084 (17)	
CH ₂ twist				1075 (156)		
CH ₂ twist + CF stretch			1083 (151)			1058 (151)
CH wag		1070 (82)	1067 (62)			
symm SO ₂ stretch*			1050 (140)			1050 (115)
CH ₂ twist	1050 (11)		1048 (42)		1040 (30)	1052 (29)
asymm SO ₂ + SN stretch			1038 (302)			1038 (292)
symm CC stretch	1035 (15)	1030 (35)		1036 (33)	1030 (63)	
CH ₂ twist	1010 (60)	1021 (42)	1022 (55)	1014 (99)		1016 (49)
CH ₂ twist			1016 (62)			
CH ₂ twist				1005 (18)		
CH ₂ twist	985 (85)			983 (102)		988 (123)
SN + SO ₂ stretch			983 (502)			983 (507)
CH ₂ wag						979 (47)
CH ₂ wag	951 (19)		966 (18)	953 (31)		962 (30)
CH ₂ wag		948 (17)		950 (35)	945 (16)	954 (26)
CH ₂ wag	934 (72)			935 (66)	933 (14)	
CH ₂ wag	894 (23)	928 (20)	913 (53)	905 (42)	930 (39)	911 (46)
CF stretch		875 (21)	866 (57)		878 (53)	893 (45)
CF stretch + CH ₂ wag		842 (89)	849 (42)		857 (51)	854 (45)
symm CC stretch	828 (15)	819 (38)	827 (29)	839 (20)		837 (45)
CF stretch + CH ₂ wag		807 (54)	807 (26)			
symm CC stretch	785 (15)		756 (29)		781 (47)	792 (25)
CH ₂ wag		746 (39)		738 (25)	734 (83)	741 (36)
symm CC + CF stretch		965 (54)			713 (61)	
CF ₂ wag	605 (19)			618 (31)		615 (49)
O... Li vibration			604 (102)			602 (75)
O... Li vibration			594 (21)			
symm O–Li–O stretch						595 (25)
NSOLiO ring vibration			579 (55)			579 (346)
F...Li vibration			570 (334)			568 (346)
CF ₂ wag	549 (32)		548 (24)	550 (52)	578 (46)	

Table 10. continued

vibrations	T1	C31	C31–Tf ₂ N [–]	Te1	C41	C41–Tf ₂ N [–]
CF ₂ wag		519 (40)				524 (29)
O–Li–O bend			526 (29)			519 (19)
F...Li vibration		525 (35)	518 (20)		484 (20)	493 (86)
		439 (52)	494 (103)		478 (83)	
		394 (49)			462 (30)	
					417 (38)	

^aThe intensities (in km/mol) are given in parentheses.

sequences of the ionic association via polymer–Li⁺ and Li⁺–anion interactions are manifested in the vibrational spectrum. The simulation vibrational frequencies are in good agreement with the experimental vibrations. The vibration assigned to the SO stretching bonds of the Li⁺–(CF₃SO₂)₂N[–] ion pair participating in the interactions with the Li⁺ ion in the presence of the polymer are predicted close to vibration at 1284 and 1266 cm^{–1} in the pure the Li⁺–(CF₃SO₂)₂N[–] ion pair. The analysis of the SO stretching vibrations confirmed that the failure of ion pair dissociation in the presence of polymer can lead to low ionic conductivity. The ionic association phenomena can be studied by employing computational vibrational spectroscopy. It would be interesting to study the ionic association of the same system in the condensed phase by performing molecular dynamics simulations.

COMPUTATIONAL METHOD

Hybrid density functional theory incorporating Becke's three-parameter exchange with Lee, Yang, and Parr's (B3LYP) correlation functional^{31,32} was used to perform the optimization on the different conformers of CH₃–(CH₂–CF₂)_n–CH₃ (*n* = 1–4) using the GAUSSIAN 16 program.³³ The internally stored 6-31G(d, p) basis set was used. Different conformers of the oligomer were generated by C–C bond rotation of CH₃–(CH₂–CF₂)_n–CH₃ (*n* = 1–4). The MESP,³⁴ *V*(*r*), at a point *r* is defined as bring a positive charge from infinity to a reference point and is given by the following equation

$$V(\mathbf{r}) = \sum_{A=1}^N \frac{Z_A}{|\mathbf{r} - \mathbf{R}_A|} - \int \frac{\rho(\mathbf{r}') d^3r'}{|\mathbf{r} - \mathbf{r}'|} \quad (1)$$

where *N* denotes the total number of nuclei in the molecule, *Z_A* is the charge of the nucleus *A* positioned at *R_A*. The first term in eq 1 refers to the bare nuclear potential and the second term represents the electronic contribution.

The MESP isosurface around the fluorine atoms are the potential binding sites of Li⁺ for the polymer and the lithium-ion was placed in the vicinity of the MESP isosurface. This geometry subsequently was optimized using the B3LYP/6-31G(d,p) method. The stationary point geometries were confirmed to be the local minima on the PES by examining the negative eigenvalues of the Hessian matrix.

ASSOCIATED CONTENT

Supporting Information

The Supporting Information is available free of charge at <https://pubs.acs.org/doi/10.1021/acsomega.1c06797>.

Zero-point corrected electronic energy and relative stabilization energy of conformers of CH₃–(CH₂–CF₂)_n–CH₃ (*n* = 1–4) are compared; optimized geometries of different conformers of Li⁺–CH₃–(CH₂–CF₂)_n–CH₃ (*n* = 1–4) (PDF)

AUTHOR INFORMATION

Corresponding Author

Nilesh R. Dhupal – Department of Chemistry and Physics, Florida Gulf Coast University, Fort Myers, Florida 33965, United States; orcid.org/0000-0001-6839-7372; Email: ndhupal@fgcu.edu

Authors

Mathew Daniel – Department of Chemistry and Physics, Florida Gulf Coast University, Fort Myers, Florida 33965, United States

Susan G. Duggan – Department of Chemistry and Physics, Florida Gulf Coast University, Fort Myers, Florida 33965, United States

Kyung Seol – Department of Chemistry and Physics, Florida Gulf Coast University, Fort Myers, Florida 33965, United States

Gregory J. McManus – Department of Chemistry and Physics, Florida Gulf Coast University, Fort Myers, Florida 33965, United States

Complete contact information is available at: <https://pubs.acs.org/10.1021/acsomega.1c06797>

Notes

The authors declare no competing financial interest.

ACKNOWLEDGMENTS

The authors acknowledge the CAS, a high-performance computational facility, Florida Gulf Coast University, for computations reported in this paper.

REFERENCES

- Xu, K. Nonaqueous Liquid Electrolytes for Lithium-Based Rechargeable Batteries. *Chem. Rev.* **2004**, *104*, 4303–4417.
- Tarascon, J. M.; Armand, M. Issues and challenges facing rechargeable lithium batteries. *Nature* **2001**, *414*, 359–367.
- Manuel Stephan, A.; Nahm, K.S. Review on composite polymer electrolytes for lithium batteries. *Polymer* **2006**, *47*, 5952–5964.
- Goodenough, J. B.; Park, K.-S. The Li-Ion Rechargeable Battery: A Perspective. *Am. Chem. Soc.* **2013**, *135*, 1167–1176.
- Wright, P. V. Electrical conductivity in ionic complexes of poly(ethylene oxide). *Polym. Int.* **1975**, *7*, 319–327.
- Johansson, P.; Gejji, S. P.; Tegenfeldt, J.; Lindgren, J. Local Coordination and Conformation in Polyether Electrolytes: Geometries of M-Triglyme Complexes (M = Li, Na, K, Mg and Ca) from ab-initio Molecular Orbital Calculations. *Solid State Ionics* **1996**, *86–88*, 297–302.
- Frech, R.; Huang, W. Polymer conformation and ionic association in complexes of lithium, sodium and potassium triflate with poly(ethylene oxide) oligomers. *Solid State Ionics* **1994**, *72*, 103–107.
- Sutjianto, A.; Curtiss, L. A. Li⁺Diglyme Complexes: Barriers to Lithium Cation Migration. *J. Phys. Chem. A* **1998**, *102*, 968–974; *J. Phys. Chem A* **1998**, *102* (6), 968–974.

- (9) Bruce, P. G.; Vincent, C. A. Polymer electrolytes. *J. Chem. Soc., Faraday Transactions* **1993**, *89*, 3187–3203.
- (10) Bhattacharja, S.; Smoot, S. W.; Whitmore, D. H. Cation and anion diffusion in the amorphous phase of the polymer electrolyte (PEO)₈LiCF₃SO₃. *Solid State Ionics* **1986**, *18–19*, 306–314.
- (11) Bi, S.; Sun, C.-N.; Zawodzinski, T. A.; Ren, F.; Keum, J. K.; Ahn, S.-K.; Li, D.; Chen, J. Reciprocated Suppression of Polymer Crystallization Toward Improved Solid Polymer Electrolytes: Higher Ion Conductivity and Tunable Mechanical Properties. *Polymer Physics* **2015**, *53*, 1450–1457.
- (12) Lascaud, S.; Perrier, M.; Vallee, A.; Besner, S.; Prud'homme, J.; Armand, M. Phase Diagrams and Conductivity Behavior of Poly(ethylene oxide)-Molten Salt Rubbery Electrolytes. *Macromolecules* **1994**, *27*, 7469–7477.
- (13) Gorecki, W.; Jeannin, M.; Belorizky, E.; Roux, C.; Armand, M. Physical properties of solid polymer electrolyte PEO(LiTFSI) complexes. *J. Phys.: Condens. Matter* **1995**, *7*, 6823.
- (14) Marzantowicz, M.; Dygas, J.R.; Krok, F.; Nowiński, J.L.; Tomaszewska, A.; Florjańczyk, Z.; Zygadlo-Monikowska, E. Crystalline phases, morphology and conductivity of PEO:LiTFSI electrolytes in the eutectic region. *J. Power Source* **2006**, *159*, 420–430.
- (15) Gejji, S. P.; Gadre, S. R.; Barge, V. J. Theoretical investigations on structure, electrostatic potentials and vibrational frequencies of diglyme and Li⁺–(diglyme) conformers. *Chem. Phys. Lett.* **2001**, *344*, 527–535.
- (16) Dhumal, N. R.; Gejji, S. P. Theoretical investigations on structure, electrostatic potentials and vibrational frequencies of Li⁺–CH₃–O–(CH₂–CH₂–O)_n–CH₃ (n = 3–7) Conformers. *Theor. Chem. Acc.* **2006**, *115*, 308–321.
- (17) Dhumal, N. R.; Gejji, S. P. Theoretical studies in local coordination and vibrational spectra of M⁺CH₃O(CH₂CH₂O)_nCH₃ (n = 2–7) complexes (M = Na, K, Mg and Ca). *Chem. Phys.* **2006**, *323*, 595–605.
- (18) Dhumal, N. R.; Gejji, S. P. Theoretical studies on blue versus red shifts in diglyme–M⁺X (M = Li, Na, K and X = CF₃SO₃, PF₆, (CF₃SO₃)₂N). *J. Phys. Chem. A* **2006**, *110*, 219–227.
- (19) Kaulgud, T. V.; Dhumal, N. R.; Gejji, S. P. Electronic Structure and Normal Vibrations of CH₃(OCH₂CH₂)_nOCH₃ M⁺(CF₃SO₃)₂N (n = 24, M = Li, Na, and K). *J. Phys. Chem. A* **2006**, *110*, 9231–9239.
- (20) Dhumal, N. R.; Gejji, S. P. Molecular interactions and vibrations in CH₃(OCH₂CH₂)₂OCH₃ M⁺X (M = Li, Na, K and X = PF₆, AsF₆, SbF₆): An ab initio study. *J. Mole. Struct. THEOCHEM* **2008**, *859*, 86.
- (21) Dhumal, N. R.; Kim, H. J.; Kiefer, J. Molecular Interactions in 1-Ethyl-3-methylimidazolium Acetate Ion Pair: A Density Functional Study. *J. Phys.chem. A* **2009**, *113*, 10397–10404.
- (22) Dhumal, N. R. Molecular interactions in 1,3-dimethylimidazolium-bis(trifluoromethanesulfonyl)imide ionic liquid. *Chem. Phys.* **2007**, *342*, 245–252.
- (23) Dhumal, N. R.; Mirjafari, A.; Kim, H. J. Deconvolution of conformational equilibria in methimazolium-based ionic liquid ion pair: Infrared spectroscopic and computational study. *J. Mol. Liq.* **2018**, *266*, 194–202.
- (24) Nishiyama, T.; Sumihara, T.; Sasaki, Y.; Sato, E.; Yamato, M.; Horibe, H. Crystalline structure control of poly(vinylidene fluoride) films with the antisolvent addition method. *Polymer J.* **2016**, *48*, 1035–1038.
- (25) Abroshan, H.; Dhumal, N. R.; Shim, Y.; Kim, H. J. Theoretical study of interactions of a Li⁺(CF₃SO₂)₂N[−] ion pair with CR₃(OCR₂CR₂)_nOCR₃ (R = H or F). *Phys. Chem. Chem. Phys.* **2016**, *18*, 6754–6762.
- (26) Dhumal, N. R.; Kim, H. J.; Kiefer, J. Electronic Structure and Normal Vibrations of the 1-Ethyl-3-methylimidazolium Ethyl Sulfate Ion Pair. *J. Phys.chem. A* **2011**, *115*, 3551–3558.
- (27) Irikura, K.; Johnson, R.; Kacker, R. Uncertainties in Scaling Factors for ab Initio Vibrational Frequencies. *J. Phys. Chem. A* **2005**, *109*, 8430–8437.
- (28) Watson, T. M.; Hirst, J. D. Density Functional Theory Vibrational Frequencies of Amides and Amide Dimers. *J. Phys. Chem. A* **2002**, *106*, 7858–7867.
- (29) Dunn, M. E.; Evans, T. M.; Kirschner, K. N.; Shields, G. C. Prediction of Accurate Anharmonic Experimental Vibrational Frequencies for Water Clusters, (H₂O)_n, n = 25. *J. Phys. Chem. A* **2006**, *110*, 303–309.
- (30) Michalska, D.; Bienko, D. C.; Abkowitz-Bienko, A. J.; Latajka, Z. Density Functional, HartreeFock, and MP2 Studies on the Vibrational Spectrum of Phenol. *J. Phys. Chem.* **1996**, *100*, 17786–17790.
- (31) Becke, A. D. Density-functional thermochemistry. III. The role of exact exchange. *J. Chem. Phys.* **1993**, *98*, 5648–5652.
- (32) Lee, C.; Yang, W.; Parr, R. G. Development of the Colle-Salvetti correlation-energy formula into a functional of the electron density. *Phys. Rev.* **1988**, *B37*, 785.
- (33) Frisch, M. J.; Trucks, G. W.; Schlegel, H. B.; Scuseria, G. E.; Robb, M. A.; Cheeseman, J. R.; Scalmani, G.; Barone, V.; Petersson, G. A.; Nakatsuji, H.; Li, X.; Caricato, M.; Marenich, A. V.; Bloino, J.; Janesko, B. G.; Gomperts, R.; Mennucci, B.; Hratchian, H. P.; Ortiz, J. V.; Izmaylov, A. F.; Sonnenberg, J. L.; Williams-Young, D.; Ding, F.; Lipparini, F.; Egidi, F.; Goings, J.; Peng, B.; Petrone, A.; Henderson, T.; Ranasinghe, D.; Zakrzewski, V. G.; Gao, J.; Rega, N.; Zheng, G.; Liang, W.; Hada, M.; Ehara, M.; Toyota, K.; Fukuda, R.; Hasegawa, J.; Ishida, M.; Nakajima, T.; Honda, Y.; Kitao, O.; Nakai, H.; Vreven, T.; Throssell, K.; Montgomery, J. A., Jr.; Peralta, J. E.; Ogliaro, F.; Bearpark, M. J.; Heyd, J. J.; Brothers, E. N.; Kudin, K. N.; Staroverov, V. N.; Keith, T. A.; Kobayashi, R.; Normand, J.; Raghavachari, K.; Rendell, A. P.; Burant, J. C.; Iyengar, S. S.; Tomasi, J.; Cossi, M.; Millam, J. M.; Klene, M.; Adamo, C.; Cammi, R.; Ochterski, J. W.; Martin, R. L.; Morokuma, K.; Farkas, O.; Foresman, J. B.; Fox, D. J. *Gaussian 16*; Gaussian, Inc.: Wallingford CT, 2016.
- (34) Gadre, S. R.; Suresh, C. H.; Mohan, N. Electrostatic Potential Topology for Probing Molecular Structure, Bonding and Reactivity. *Molecules* **2021**, *26*, 3289.